

Glass-ceramics with random and oriented microstructures

Part 3 *The preparation and microstructure of an aligned glass-ceramic*

D. I. H. ATKINSON*, P. W. McMILLAN
Department of Physics, University of Warwick, Coventry, UK

The technique of hot extruding a glass-ceramic to produce a material with an aligned crystal microstructure is described. The results of a statistical investigation to analyse the degree of morphological orientation of an extruded glass-ceramic based on the $\text{Li}_2\text{O}-\text{SiO}_2$ system are reported. Details are also presented of the determination of the crystallographic orientation in the aligned glass-ceramic.

1. Introduction

When a glass-ceramic is devitrified under conditions where no external constraints are applied to it, the crystalline phase in the bulk material is randomly oriented in a glassy matrix [1]. Surface crystallization can produce an ordered microstructure within the boundary layer of the glass-ceramic [2, 3]. This preferred crystal orientation at the surface of the material results from the anisotropy of the growth rates; although the crystals at the nucleating surface may be randomly oriented, the crystals oriented with the fast growth direction perpendicular to the surface take precedence.

In a glass-ceramic the crystalline phase may be aligned with respect to the crystal planes or the morphology of the crystals or both. The morphological orientation of the crystal requires that the crystalline phase is asymmetric and therefore no such orientation could be detected in a system of spherical crystals.

Extrusion is a well documented process in the technology of metals and plastics for the manufacture of rods, tubes or other profiles [4-6]. In composite materials, in which a second phase is mixed with the matrix, an extrusion technique can be used to align this phase [7]. The flow behaviour of glasses when they are hot-extruded has been investigated by Roeder [8,9].

Ashbee [10, 11] has reported on the production of an anisotropic glass-ceramic by extruding

the glass through opposed dies at a temperature near the crystallization temperature. The present authors have briefly reported on some results obtained from hot-extruding a glass-ceramic [12]. In the present paper the apparatus used for the extrusion technique and the resulting glass-ceramic microstructure are described.

There are two distinct methods of extrusion; directed and inverted extrusion. In the work reported, a glass-ceramic was hot extruded using the direct extrusion method. In this technique a billet of material, contained in a cylinder, is compressed by a plunger or punch, which forces the material through a die aperture. The cross-sectional area of the die aperture is less than that of the initial billet and the cross-section of the extruded product is determined by the shape of this aperture. During the direct extrusion process the punch and the extruded rod move in the same direction.

2 Hot extrusion

2.1. Methods and materials

The equipment which was developed to extrude a glass-ceramic does not differ significantly from that used for extruding metals or plastics. The apparatus which is shown in Figs. 1 and 2 consists of a stainless steel plunger with a water jacket which is attached to the cross-head of an Instron Universal testing machine. The plunger descends

*Present address: Metal Box Ltd., Physics Section, London NW10, UK.

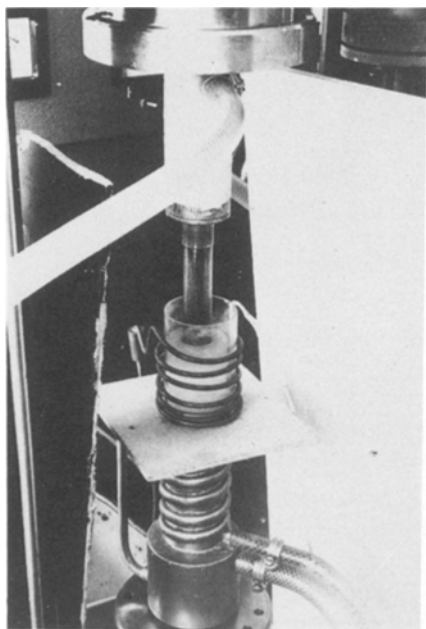


Figure 1 Photograph of the extrusion apparatus.

into a die which is heated by high frequency induction and stands on the load cell of the Instron machine. The induction coil is electrically insulated from the die by a fused silica tube. The temperature of the die can be monitored by optical pyrometry or by a thermocouple which is situated in the die near the aperture. When the extruded material is clear of the die it enters a water-cooled collection zone; the die is a loose fit on the stand at room temperature and can be lifted off to collect the extruded material.

For a given extrusion velocity the applied punch pressure is a function of the frictional forces between the die walls and the billet and the ratio of the cross-sectional areas of the container and die channel. The aperture angle of the die will determine the flow pattern of the material in the die; an aperture angle of 180° will produce areas of stagnant flow in the corners of the die. The dies used for all the extrusion experiments had the following parameters:

- diameter of die channel, 0.25 in. (6.35 mm)

- length of die channel, 0.75 in. (19.05 mm)

- aperture angle of die, 90°

- ratio of the cross-sectional areas of the container and die channel, 16:1.

The die channel and the container are of circular cross-section so that the temperature distribution inside the die possesses circular symmetry. If this is not the case the extruded material will

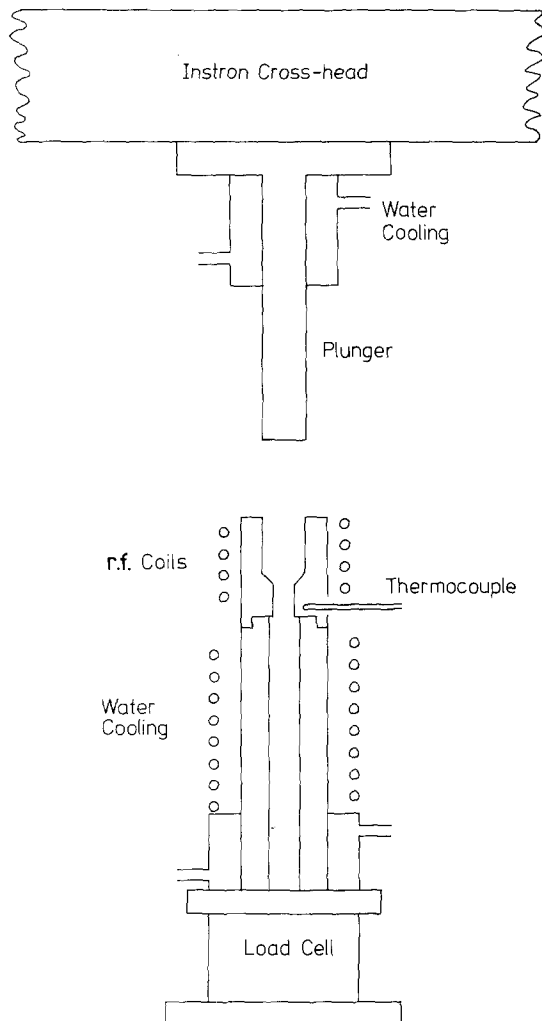


Figure 2 Schematic diagram of the extrusion apparatus.

leave the die channel obliquely. The extrusion dies were constructed from a high strength, heat-resisting nickel-base alloy (Inconel Alloy 600).

The extrusion apparatus can be operated in two models. Extrusion can be achieved by maintaining a constant pressure on the sample in the die and varying the rate of descent of the plunger, or the rate of descent of the plunger can be maintained at a constant value and the applied pressure allowed to vary accordingly. When the plunger is applying a load to the glass-ceramic which is to be extruded, the stress is relieved by material flowing through the aperture of the die. A certain amount of material is extruded in the reverse direction between the wall of the container and the plunger. This "back-extruded" material helps to lubricate the plunger in the container and prevent the apparatus siezing (Fig. 3).

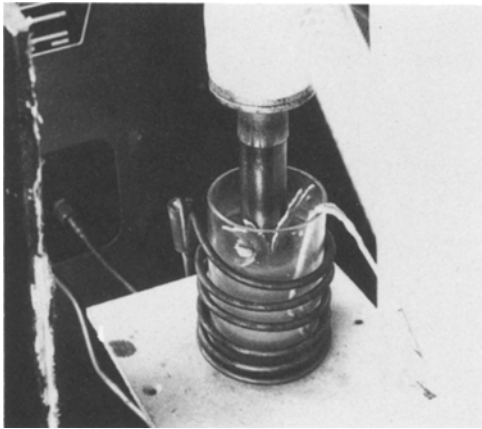


Figure 3 Back extrusion.

To extrude a glass-ceramic, a glass billet was placed in the die and heat-treated *in situ* for a pre-determined period of time at a set temperature to produce a glass-ceramic. When the specimen had been heat-treated the plunger was lowered into the die and the extrusion process carried out in one of the two modes described above. The temperature of the die was maintained at the constant value of the heat-treatment throughout the extrusion process. The constant pressure method of operation was found to be easiest to perform experimentally.

2.2. Flow behaviour during extrusion

Roeder [8] has studied the flow of a glass during extrusion through circular die apertures and has

shown that under certain conditions this flow obeys the Hagen–Poiseuille law, which describes the flow of viscous liquids through capillaries. The Hagen–Poiseuille law states that for an incompressible Newtonian fluid, the isothermal laminar volumetric flow rate V , is given by:

$$V = \frac{\pi \Delta p r^4}{8 \eta l} \quad (1)$$

where Δp is the pressure difference between the entrance and exit of the tube, and r and l are its radius and length respectively; η is the viscosity of the liquid. Frictional forces at the walls of the tube produce an inhomogeneous distribution of flow velocity v across the tube; a completely stagnant layer at the die walls produces a parabolic velocity profile:

$$v = \frac{\Delta p}{4 \eta l} (r^2 - x^2) \quad (2)$$

where x is a radial component. The maximum velocity is at the axis of the tube ($x = 0$) and the velocity is zero at the walls ($x = r$).

To determine the flow of material through the die a billet consisting of alternate layers of a glass-ceramic and cupric oxide was extruded at 830°C . The resulting section cut parallel to the extrusion axis of the rod is shown in Fig. 4.

At any moment during the extrusion process the distortion of the dark interface (cupric oxide) reveals the course of the glass-ceramic flow. It can be seen that the material flows faster in the inner zone than at the edge; analysis of this extrusion

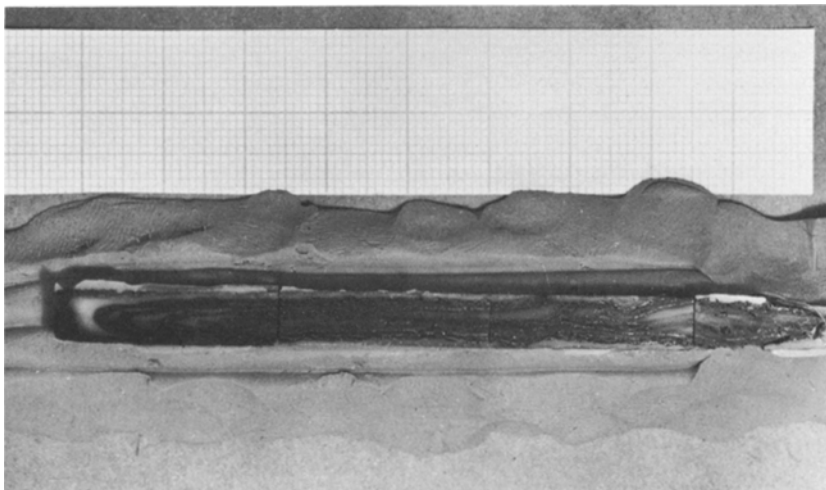


Figure 4 The result of extruding alternate layers of a glass-ceramic and cupric oxide (black) (the small squares are $1 \text{ mm} \times 1 \text{ mm}$).

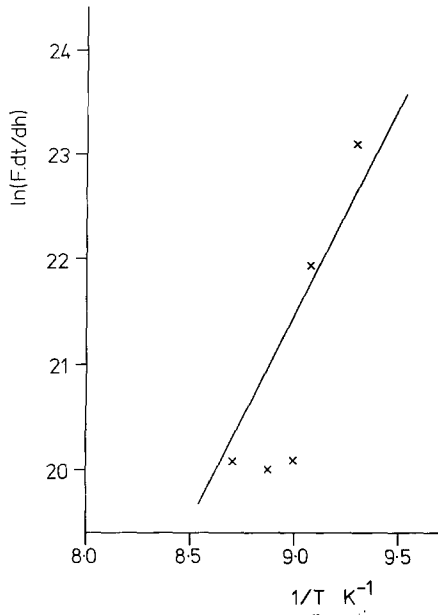


Figure 5 The variation of $F \cdot (dt/dh)$ with temperature for the extrusion of the glass-ceramic.

indicates that the flow pattern is in good agreement with the Hagen–Poiseuille law.

2.3. Extruding a glass-ceramic

The statistical description and properties of a glass-ceramic with a random crystal microstructure have been previously reported by the authors [13, 14]. This glass-ceramic based on the $\text{Li}_2\text{O}-\text{SiO}_2$ system was extruded in the approximate temperature range 800 to 880° C, with an applied load of 2500 to 100 kg. At each extrusion temperature the original glass billet was heat-treated for 30 min in the die before the pressure was applied; each extrusion lasted approximately 2 h. The rate of descent of the plunger and the temperature of the die were monitored during an extrusion experiment. From a consideration of Equation 1 it can be seen that the rate of descent of the plunger (dh/dt), is related to the applied load on the plunger, F , by:

$$\frac{dh}{dt} \propto \frac{F}{\eta} \quad (3)$$

The viscosity-temperature function for a glass is of the form [15]:

$$\eta = A \exp\left(\frac{E}{RT}\right) \quad (4)$$

where A and E are constants, E being a measure of the activation energy for viscous flow, R is the gas

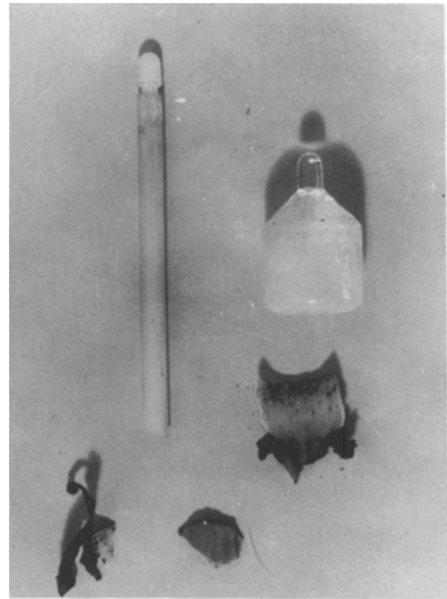


Figure 6 The original glass billet (approximately 1 in. diameter), the extruded rod and the back extruded material.

constant and T the temperature in degrees Kelvin. If this equation is combined with the relationship above then:

$$\exp\left(\frac{E}{RT}\right) \propto F \cdot \frac{dt}{dh} \quad (5)$$

Fig. 5 is a graph of $\ln[F(dt/dh)]$ versus the inverse of the absolute temperature for the extrusion of the glass-ceramic; the gradient of the line provides a measure of the activation energy:

$$E = (79 \pm 28) \text{ kcal mol}^{-1}.$$

In the extrusion of the glass-ceramic through the die the diameter of the product was the same as that of the die aperture; the surface of the extruded rod was smooth and no evidence was found of the die material diffusing into the glass-ceramic. Fig. 6 shows the original glass billet (approximately 1 in., 25.4 mm, diameter), the extruded rod and the back extruded material.

3. The microstructure of the extruded material

3.1 Introduction

Fig. 7 shows typical scanning electron micrographs of the structure produced by extruding the glass-ceramic; (a) and (b) are of sections respectively

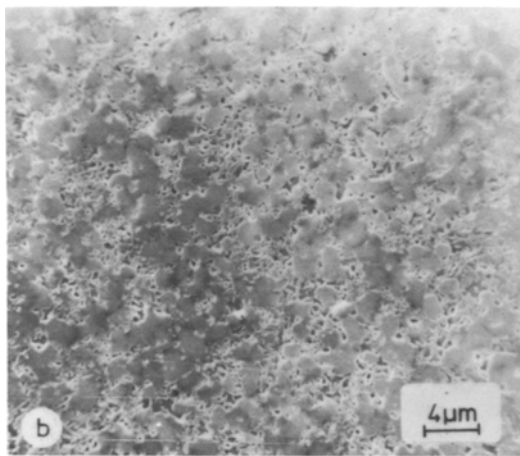
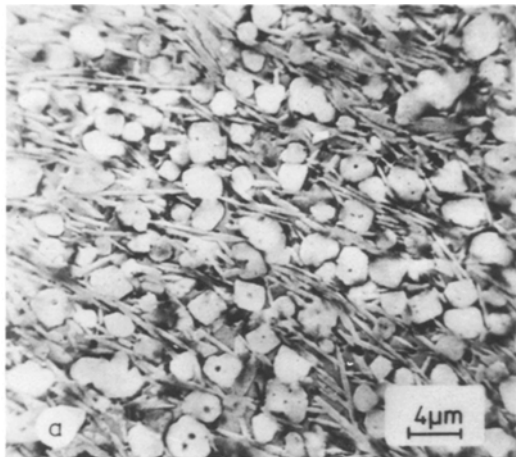


Figure 7 SEM micrograph of the extruded rod (a) parallel and (b) perpendicular to the extrusion axis.

parallel and perpendicular to the extrusion axis. These micrographs show that the resulting glass-ceramic contained two different crystal morphologies. X-ray diffraction of powdered specimens indicated that lithium disilicate and tridymite crystalline phases were present. The needle-shaped disilicate phase is morphologically oriented parallel to the extrusion axis and in the case where the tridymite crystals have a non-unitary aspect ratio these show a similar orientation.

In all the areas of the extruded specimens examined at high magnification a marked difference was evident between the parallel and perpendicular sections of the material. The micrographs indicate that the tridymite crystal phase, which in some cases occupies a greater volume fraction than the disilicate phase, produces an inferior alignment.

3.2. Statistical analysis of the morphological orientation

The variation of the microstructure with position in the extruded rod was analysed statistically in terms of the volume fraction of the crystalline phases, the mean crystal-crystal spacing [13] and the degree of orientation of the crystals. The degree of orientation was evaluated using a technique based on the work of Hiliard [16]. To analyse a micrograph a test grid consisting of four parallel and equally spaced chords of a circle was rotated about the centre of the circle. The number of intersections with crystal boundaries on the micrograph was counted at twelve orientations at 15° increments. The data of the number of intersections per line length of the test grid for a given angle were then analysed to determine the width of the angular distribution curve of the number of crystals versus angle [17]. In this analysis no distinction was made between the two different crystal phases present in the material and the numbers describing the microstructure were evaluated on sections parallel and perpendicular to the extrusion axis.

The angular distribution function was determined in a number of places on sections through and parallel to the extrusion axis; these data are represented in Fig. 8 by vectors drawn on a



Figure 8 A schematic diagram of the variation of the angular distribution function in the extruded material.

schematic diagram of this section for an extrusion experiment. The end-point of each of these vectors is at the approximate positions of the area which was analysed and it points in the direction of the maximum value of the angular distribution curve. The magnitude of the vector is inversely proportional to the width of the distribution function. It is evident from Fig. 8 that the extruded glass-ceramic contains an aligned crystal microstructure, the magnitude of which is independent of the quantity of material extruded. The orientation is symmetrical about the axis of the rod and the direction of the vectors suggests that the direction of the maxima of the distribution curves are tangents to parabolas drawn on the section. This concept of parabolas is consistent with the Hagen-Poiseuille flow of a Newtonian fluid down a tube. The minimum value of the angular spread of the major axes of the crystals with the extrusion axis in the material was 40° and the maximum was 60° ; a randomly oriented specimen is defined as one which has an angular spread of 180° . The largest degree of orientation (corresponding to the minimum angular spread) was found to be at the surface of the material where the greatest flow velocity gradient exists; the smallest degree existed in the centre of the extruded rod. Sections perpendicular to the extrusion axis had a random microstructure.

The variation of the volume fraction V_f , of both crystal phases with the extrusion temperature is shown in Fig. 9. The mean crystal-crystal spacing λ , in this material was measured in directions parallel and perpendicular to the extrusion

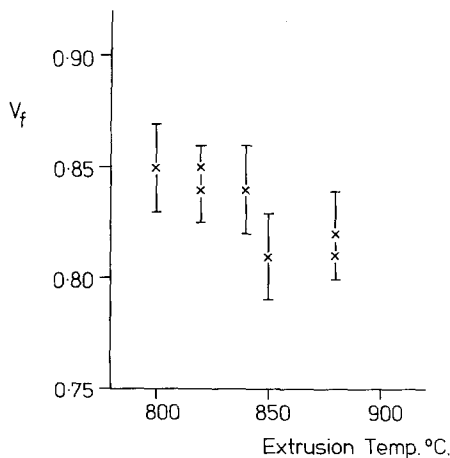


Figure 9 The variation of the volume fraction V_f , with the extrusion temperature.

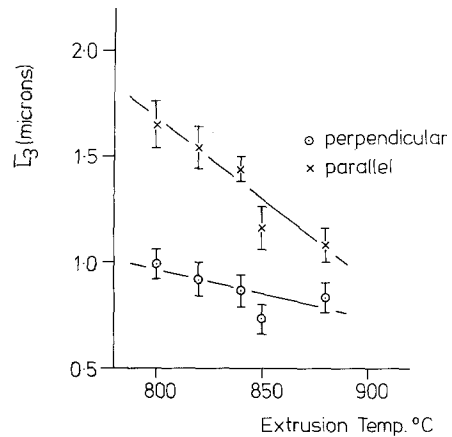


Figure 10 The variation of the mean crystal size \bar{L}_3 , with the extrusion temperature.

axis and was found to be constant. In the radial direction it had a value of:

$$\lambda_R = 0.17 \pm 0.03 \mu\text{m}$$

and parallel to the extrusion axis:

$$\lambda_P = 0.28 \pm 0.04 \mu\text{m}.$$

The difference between these values is a reflection of the different pressure gradients which exist in the material whilst it is being extruded.

No radial or axial length dependence of the volume fraction or mean crystal-crystal spacing was detected in the samples extruded. The variation of the mean crystal size \bar{L}_3 , with the extrusion temperature is shown in Fig. 10; in this graph the lengths of the crystals were evaluated in directions parallel and perpendicular to the extrusion axis. At a given extrusion temperature the ratio of these two lengths is the mean aspect ratio of the crystals present in the glass-ceramic; if this ratio has a value of one the crystals are isometric.

3.3. Crystallographic orientation

Rindone [3] has measured a preferred crystallographic orientation of lithium disilicate crystals in the surface of a glass-ceramic specimen using a X-ray technique. The crystals formed with their (002) planes parallel to the surface; in the bulk of the material the crystals were randomly oriented.

The crystallographic orientation of the lithium disilicate crystals in the extruded specimens was determined by an X-ray diffraction technique. Polished and lightly etched specimens cut parallel and perpendicular to the extrusion axis were

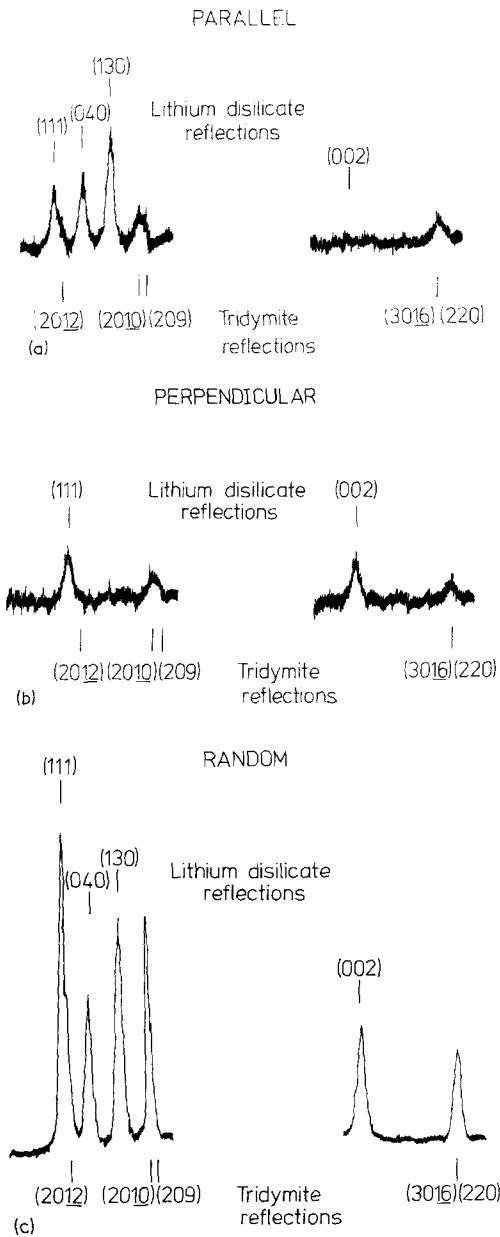


Figure 11 The reflected X-ray intensity from (a) a sample cut parallel and (b) perpendicular to the extrusion axis; (c) shows the intensity from a random arrangement of crystals.

irradiated with a cobalt $K\alpha$ beam of X-rays and the deflected intensity was recorded. A standard two circle diffractometer was used and the sample were mounted in an amorphous cold setting resin.

The intensity of the (hkl) reflections were measured relative to that from the (111) planes of the disilicate phase in each sample. Fig. 11a and b are part of the reflected X-ray intensity from

TABLE I A summary of the reflected X-ray intensities from the lithium disilicate crystal phase

(hkl)	Random $I_{(hkl)}/I_{(111)}$	Parallel $I_{(hkl)}/I_{(111)}$	Perpendicular $I_{(hkl)}/I_{(111)}$
(111)	100	100	100
(130)	~ 60	~ 200	v. weak
(040)	~ 50	~ 150	v. weak
(002)	~ 30	v. weak	~ 80

specimens cut parallel and perpendicular to the extrusion axis. The diffracted intensity from a specimen with a random arrangement of crystals is shown in Fig. 11c; the Bragg reflections from this specimen are more intense because a larger area of the sample was irradiated compared with the extruded samples.

A comparison of these figures shows that the (040) and (130) reflections from the lithium disilicate phase are missing from the specimen cut perpendicular to the axis. In the case of the parallel sample, the (002) reflection is very weak or non-existent. The values of the reflected intensity from the (hkl) planes relative to that from the (111) planes for the lithium disilicate phase are summarized in Table I. A consideration of these data show that the disilicate crystals are crystallographically aligned with the 001 direction parallel to the extrusion axis; the tridymite phase shows no such orientation.

4. Discussion

The results obtained from the statistical analysis of the microstructure of the extruded specimens indicate that the crystalline phases in the material are morphologically aligned with their major axes parallel to the extrusion axis. The X-ray diffraction experiments shows that the lithium disilicate phase was also oriented with the c crystallographic axis parallel to the extrusion axis; however, the material has no bulk preferred orientation with respect to the a or b directions in the crystal.

A study of the surface crystallization in control specimens of the glass-ceramic showed that the lithium disilicate crystals were formed with the (002) planes parallel to the surface; the long axis of the crystal being the 001 direction. These data correlate with the determination of the major axis of the disilicate phase in the extruded specimens.

The statistical analysis was carried out on micrographs of small areas of the material whereas in the X-ray diffraction experiments all of the section of the extruded specimen was used. It can

be concluded from this that the extruded material exhibits a bulk orientation of the lithium disilicate crystal phase.

The mechanism which causes the crystal orientation is not easy to analyse; shear alignment and crystal-crystal interactions are involved in the process. Several authors have considered the alignment of rigid cylinders immersed in a sheared viscous fluid [18–20]. A particle which is not lying with its major axis parallel to the flow direction experiences an angular velocity about its centre of mass and a translational velocity parallel to the flow direction. The angular velocity causes the particle to rotate towards an orientation parallel to the direction of flow. For a system of non-interacting particles a preferred orientation of particles parallel to the axis of flow can be shown to exist.

The glass-ceramics which were extruded had a volume fraction in excess of 0.80 and crystal-crystal interactions in this system must occur. The extrusion of a glass-ceramic and the subsequent crystal alignment can be likened to the flow of logs down a river; the logs flow with their major axis pointing down river and log-log interactions do occur but a preferred orientation of logs is maintained.

Acknowledgement

The authors wish to thank the SRC for financial support.

References

1. P. W. McMILLAN, "Glass-ceramics" (Academic Press, London, 1964).
2. C. L. BOOTH and G. E. RINDONE, *J. Amer. Ceram. Soc.* **47** (1964) 25.
3. G. E. RINDONE, in "Symposium on Nucleation and Crystallization in Glasses and Melts", edited by M.K. Reser, G. Smith and H. Ingsley (Am. Ceram. Soc. Inc., Columbus, Ohio, 1962).
4. R. CHADWICK, *Met. Rev.* **4** (1959) 189.
5. C. E. PEARSON and R. N. PARKINS, "The Extrusion of Metals" (Chapman and Hall London, 1960).
6. E. C. BERNHARDT, "Processing of Thermoplastic Materials" (Reinhold, New York; Chapman and Hall, London, 1959).
7. R. W. JECH, E. P. WEBER and A. D. SCHWOPE, in "Reactive Metals", edited by W. R. Clough (Interscience, 1959).
8. E. ROEDER, *J. Non-Crystalline Solids* **5** (1971) 377.
9. *Idem, ibid* **7** (1971) 203.
10. K. H. G. ASHBEE, *Nature* **252** (1974) 469.
11. *Idem, J. Mater. Sci.* **10** (1975) 911.
12. D. I. H. ATKINSON and P. W. McMILLAN, *ibid* **10** (1971) 612.
13. *Idem, ibid* **11** (1976) 989.
14. *Idem, ibid* **11** (1976) 994.
15. J. E. STANWORTH, "Physical Properties of Glass" (Oxford, London, 1950).
16. J. E. HILLIARD, *Trans. AIME* **224** (1962) 1201.
17. D. I. H. ATKINSON, Ph.D. Thesis, University of Warwick (1975).
18. G. B. JEFFERY, *Proc. Roy. Soc. London.* **A102** (1923) 161.
19. S. G. MASON and R. St. J. MANLEY, *ibid* **A238** (1956) 117.
20. E. ANCZUROWSKI and S. G. MASON, *Trans. Soc. Rheol.* **12** (1968) 209.

Received 8 June and accepted 7 July 1976.